Kowalczyk, P. S., & di Bernardo, M. (2003). Two-parameter sliding bifurcations of limit cycles in Filippov Systems.

Early version, also known as pre-print

Two–parameter Sliding Bifurcations of Limit Cycles in Filippov Systems

P. Kowalczyk*, M. di Bernardo †

June 30, 2003

Abstract

This paper is concerned with the extension of the theory of sliding bifurcations in Filippov systems to the case of codimension-two degenerate sliding bifurcations. The analysis is carried out for generic n-dimensional piecewise smooth systems. The possible degenerate scenarios are classified and unfolded. It is shown that several branches of codimension-one sliding bifurcations originate from each of the degenerate codimension-two point. Such branches are appropriately classified. A friction oscillator is used as a representative example to illustrate and confirm the theoretical derivations.

PACS codes: 05.45.+b, 02.30.Hq, 03.20.+i, 84.30.Ng
keywords: bifurcation, piecewise smooth, sliding, grazing

1 Introduction

Nonsmooth dynamical systems have been shown to exhibit many bifurcation phenomena that cannot be explained in terms of classical bifurcation theory for smooth systems [1, 7]. In particular, the existence of a new class of bifurcations, or C-bifurcations, has been suggested for these systems. C-bifurcations involve nontrivial interactions between the system Ω-limit set and phase-space boundaries where the system vector field (or state) is discontinuous.

They can be classified in *border-collisions* [19, 6] if they involve fixed points of nonsmooth maps or *grazings* [18] if limit cycles in nonsmooth flows are considered. While in the former case, under parameter variations a fixed point crosses the nonsmooth boundary, in the latter a limit cycle becomes tangential to it. Recently, it was shown that border-collisions and grazings can be unified by considering a set of appropriate normal form maps (see [4] for further details).

Instances of these bifurcations have been found in many systems of relevance in applications. Experimental observations of C-bifurcations were reported in power electronics circuits, mechanical systems etc. [1].

Systems with discontinuous vector fields (or Filippov systems) were recently shown to exhibit a novel class of C-bifurcations termed as *sliding bifurcations* [11]. Namely, these bifurcation phenomena occur when the limit cycle of a nonsmooth system interacts with a region of the switching manifold which is

* *Corresponding Author.* Department of Engineering Mathematics, University of Bristol BS8 1TR U.K. Tel. +44(0)117 9289798; fax +44(0)117 9251154 E-mail: p.kowalczyk@bristol.ac.uk

†Department of Engineering Mathematics, University of Bristol BS8 1TR U.K. m.dibernardo@bristol.ac.uk

simultaneously attracting from both of its sides. When this occurs, in the simplest case, the orbit has been shown to acquire an additional segment of trajectory lying within such a region (or sliding motion). Sliding bifurcations were recently shown to be the cause for the onset of complex transitions to stick-slip periodic behaviour and chaos in frictionoscillators [10].

Most of the existing theory of C-bifurcations deals with the case of codimension-1 events, observed under variation of one bifurcation parameter. As recently highlighted in [13], there is the need to extend the theory to encompass the case of codimension-two bifurcations. The only mention to these events found in the literature was reported in [12]. Rather than being a mere academic exercise, the classification and unfolding of such codimension-two bifurcations is essential to construct appropriate branching routines to be used for the numerical continuation of limit cycles in Filippov systems. As will be shown later in Sec. 6, for example, codimension-two phenomena are found to organise the bifurcation diagrams of friction oscillators.

A first attempt to classify the possible codimension-two scenarios involving C-bifurcations can be found in [13, 14]. In this paper, we focus on the case of codimension-two sliding bifurcations, i.e. bifurcations associated to the degeneracy of one of the analytical conditions characterising codimension-one sliding bifurcations [11]. In particular, starting with a brief overview of codimension-one sliding bifurcations, in Sec. 3 and 4 we present a first classification of degenerate sliding bifurcations, carrying out a local unfolding of each different case. We show that locally to the codimension-two bifurcation point, several different codimension-1 scenarios are possible. Using a combination of asymptotics and Taylor series expansions, analytical approximations of phase-space boundaries between regions associated to different qualititative behaviour are found in Sec. 5 . Such boundaries are then used to unfold the codimension-two bifurcation in parameter space.

Branches of codimension-1 sliding bifurcations are shown to originate from the codimension-two point and are classified through the investigation of the local phase-space topology and the derivation of appropriate normal form maps. For the sake of brevity, the analysis is detailed for one of the four possible cases. A friction oscillator is used in Sec. 6 as a representative example to illustrate and confirm the theoretical derivations.

1.1 Systems of interest

We focus our attention on systems with discontinuous vector fields. Such systems are characterised by the presence of discontinuity boundaries in phase space between regions where the vector field is smooth and continuous. We consider a sufficiently small region $D \subset \mathbb{R}^n$ of phase space where the equations governing the system flow can be written as:

$$\dot{x} = \begin{cases} F_1(x,\mu) & \text{for} \quad H(x) > 0, \\ F_2(x,\mu) & \text{for} \quad H(x) < 0, \end{cases} \tag{1}$$

where F_1, F_2 are sufficiently smooth vector functions and $H(x)$ is some scalar function depending on the system states. D is split into two subspaces, say G_1 and G_2, with smooth and continuous dynamics. The discontinuity boundary between G_1 and G_2 we assume to be a smooth hyperplane, say Σ. Namely:

$$G_1 := \{x \in \mathbb{R}^n : H(x) > 0\}, \tag{2}$$

$$G_2 := \{x \in \mathbb{R}^n : H(x) < 0\}, \tag{3}$$

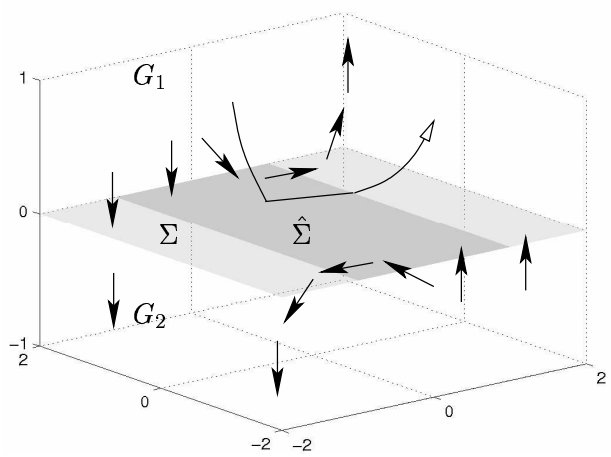

Figure 1: Phase space topology of a system with discontinuous vector fields

$$\Sigma := \{x \in \mathbb{R}^n : H(x) = 0\}. \tag{4}$$

The resulting topology in the case of a representative three-dimensional phase space is shown schematically in Fig. 1. If the vector fields point towards Σ from both subspaces G_1 and G_2, a trajectory hitting Σ is forced to evolve within the discontinuity set until reaching some point on it where one of the two vector fields, F_1 or F_2, changes its direction (the boundary of the shaded region in Fig. 1 denoted by $\hat{\Sigma}$). The solution which lies within the system discontinuity set is termed as sliding motion and the region of the discontinuity set where such a motion may occur is labelled *sliding region*. Throughout this region the following condition must hold:

$$\langle \nabla H, F_2 \rangle - \langle \nabla H, F_1 \rangle > 0, \tag{5}$$

where ∇H denotes a vector which is normal to Σ and $\langle \nabla H, F_i \rangle$ is the projection of the vector field F_i along the normal to Σ.

Following Utkin's equivalent control method [20], we can derive the vector field F_s which governs the flow within the sliding region as a vector function belonging to the convex hull of F_1 and F_2, defined by:

$$F_s = \frac{F_1 + F_2}{2} + H_u \frac{F_2 - F_1}{2}, \tag{6}$$

where $-1 \leq H_u \leq 1$. $H_u(x)$ can be obtained in terms of F_1 and F_2 by considering that F_s must be tangential to the switching manifold, i.e. $\langle \nabla H, F_s \rangle = 0$. Using this condition, we then have

$$H_u(x) = -\frac{\langle \nabla H, F_1 \rangle + \langle \nabla H, F_2 \rangle}{\langle \nabla H, F_2 \rangle - \langle \nabla H, F_1 \rangle}. \tag{7}$$

We can now define the sliding region as:

$$\hat{\Sigma} := \{x \in \Sigma : |H_u(x)| < 1\}, \tag{8}$$

and its boundaries as:

$$\partial \hat{\Sigma}^- := \{x \in \Sigma : H_u(x) = -1\}, \tag{9}$$

$$\partial\hat{\Sigma}^{+} := \{x \in \Sigma : H_u(x) = 1\}. \tag{10}$$

The normal vector to the boundary $\partial\hat{\Sigma}^{-}$ can be expressed in terms of vector fields F_1, F_2 and ∇H (see [11] for details) yielding:

$$\nabla H_u = -\frac{2}{\langle \nabla H, F_2 \rangle} \nabla H \frac{\partial F_1}{\partial x}. \tag{11}$$

The denominator of (11) is positive which follows from (5) and (8).
Without loss of generality, we assume that both Σ and $\partial\hat{\Sigma}^{-}$ can be flattened by making a series of appropriate near-identity transformations (for further details see [11]).

2 One-parameter Sliding Bifurcations

Codimension-1 sliding bifurcations of limit cycles, termed also as global sliding bifurcations [17] have been extensively studied in the literature [8, 16, 15, 11]. It has been shown that there are four distinct types of codimension-1 sliding bifurcations [16, 15, 11] which may lead to dramatic dynamical scenarios [10].

We refer the reader to [11] for a detailed description of codimension-1 sliding bifurcations as well as for the normal form map derivations. A schematic picture of all the possible cases is shown in Fig. 2. We assume w.l.o.g. that every

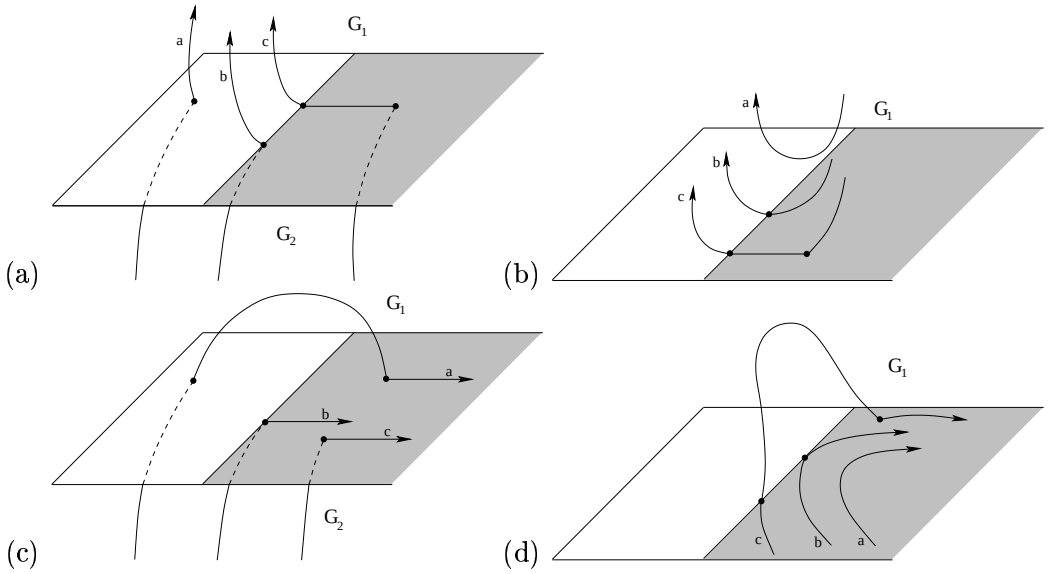

Figure 2: The four possible bifurcation scenarios involving collision of a segment of the trajectory with the boundary of the sliding region $\partial\hat{\Sigma}^{-}$. (a) crossing-sliding; (b) grazing-sliding; (c) switching-sliding; (d) adding-sliding.

bifurcation scenario takes place at the boundary of the sliding region, $\partial\hat{\Sigma}^{-}$, and is at the origin in some local set of coordinates.

The grazing sliding, crossing sliding and switching sliding cases (in [11] crossing sliding is termed as sliding type I and switching sliding as sliding type II)

are determined by conditions[1][11]:

$$\nabla H(x^*) \neq 0, \tag{12}$$

$$\langle \nabla H, F_1^* \rangle = 0, \tag{13}$$

$$\langle \nabla H, \frac{\partial F_1^*}{\partial x} F_1^* \rangle \neq 0. \tag{14}$$

Condition (12) states that Σ is a well defined manifold, (13) implies that at the bifurcation the vector field is tangential to Σ and, finally, (14) implies that the vector field points outside or inside of the sliding region $\hat{\Sigma}$.

Let us now consider the fourth case namely what happens when the bifurcating trajectory is contained in the sliding set $\hat{\Sigma}$ and undergoes a bifurcation. In the codimension-1 case this amounts to the adding-sliding scenario (see [11] for the description of the adding sliding bifurcation which was termed in the aforementioned work as the multisliding bifurcation). The adding sliding scenario is determined by conditions (12), (13) with

$$\langle \nabla H, \frac{\partial F_1^*}{\partial x} F_1^* \rangle = 0 \tag{15}$$

$$\langle \nabla H, \left(\frac{\partial F_1^*}{\partial x} \right)^2 F_1^* \rangle < 0 \tag{16}$$

3 Codimension-2 Degenerate Sliding Bifurcations

Now, we focus our attention on the possible cases of higher codimension sliding bifurcations. Namely, we consider those bifurcations which are originated from the violation of one of the nondegeneracy conditions at a codimension-1 sliding bifurcation point, namely conditions (14) or condition (16). Thus, the work presented in what follows is an extension of the analysis of sliding bifurcations presented in [11].

[1]superscript * denotes quantities evaluated at the bifurcation point which is set at the origin

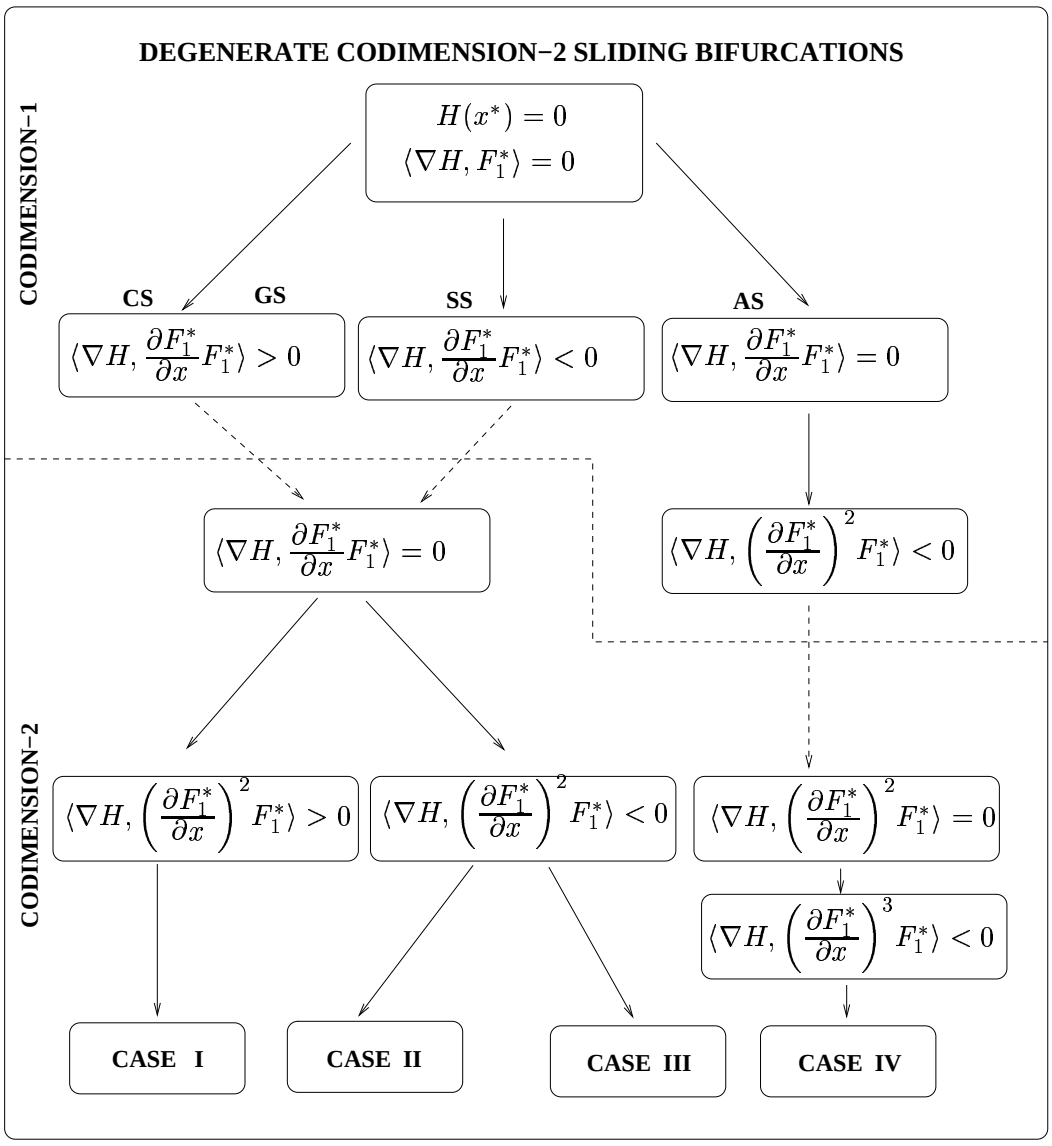

Figure 3: Classification tree of different degenerate codimension-2 sliding bifurcations

Degeneracy of condition (14) leads to

$$\langle \nabla H, \frac{\partial F_1^*}{\partial x} F_1^* \rangle = 0. \tag{17}$$

which states that at the bifurcation point the vector field is tangential to $\partial \hat{\Sigma}^-$. An additional condition on the curvature of the vector field with respect to the boundary of the sliding region determines the possible codimension-2 sliding bifurcation scenarios.

In particular, we can distinguish the following instances:

- **degenerate crossing-sliding:**

$$\langle \nabla H, \left(\frac{\partial F_1^*}{\partial x}\right)^2 F_1^* \rangle > 0, \tag{18}$$

- **degenerate grazing- or switching-sliding:**

$$\langle \nabla H, \left(\frac{\partial F_1^*}{\partial x}\right)^2 F_1^* \rangle < 0 \tag{19}$$

We classify as codimension-2, sliding bifurcations determined by conditions (12), (13), (17) and (18) or (19), because one additional independent parameter variation is required to make condition (14) degenerate. Note, that, generically, the case when the quantity in (18) and (19) is 0 would imply another degeneracy and in consequence would be a codimension-3 event. This is true unless the bifurcating trajectory evolves within the switching manifold approaching the codimension-2 node from within $\hat{\Sigma}$. Thus, considering the case:

$$\langle \nabla H, \left(\frac{\partial F_1^*}{\partial x}\right)^2 F_1^* \rangle = 0. \tag{20}$$

the bifurcation scenario will be determined by an additional condition which describes the change of the curvature at the bifurcation point. Since, it was assumed that the sliding bifurcation occurs on the boundary $\partial\hat{\Sigma}^-$, the additional condition determining the degenerate bifurcation event in this case reads:

- **degenerate sliding-adding:**

$$\langle \nabla H, \left(\frac{\partial F_1^*}{\partial x}\right)^3 F_1^* \rangle < 0. \tag{21}$$

Should we consider the boundary $\partial\hat{\Sigma}^+$, conditions for codimension-2 sliding bifurcations (18), (19), (21) would yield an opposite sign.

4 Main Results

We now summarise the main features of our derivation for each of the degenerate cases under investigation. Namely, we will:

1. outline the local phase space portrait corresponding to the analytical conditions for each of the codimension-two bifurcation points;
2. illustrate the unfolding in parameter space around each of these points;

For the sake of clarity, we will detail in Sec. 5 how these features were obtained and analysed by taking one of the four codimension-two cases as a representative example. It is worth mentioning here that similar analytical derivations can be given for each of the other cases.

4.1 Case I: Degenerate Crossing-Sliding

We shall start our considerations with the codimension-2 scenario associated to conditions (12),(13), (17) and (18). The vector field at the bifurcation point is tangential to the switching manifold Σ (condition (13)) and to the boundary $\partial\hat{\Sigma}^-$ (condition (17)). Additionally, the trajectory is characterised by a local maximum with respect to this boundary (condition (18)). The phase space portrait locally to the bifurcation point is schematically depicted in Fig. 4.

Locally to the codimension-two bifurcation point, different perturbations will lead to the formation of different types of trajectories. For instance, the trajectory labelled as $T1$ in Fig. 4 will contain an additional segment of sliding motion, while the one labelled as $T2$ will additionally present an extra section of trajectory in region G_1.

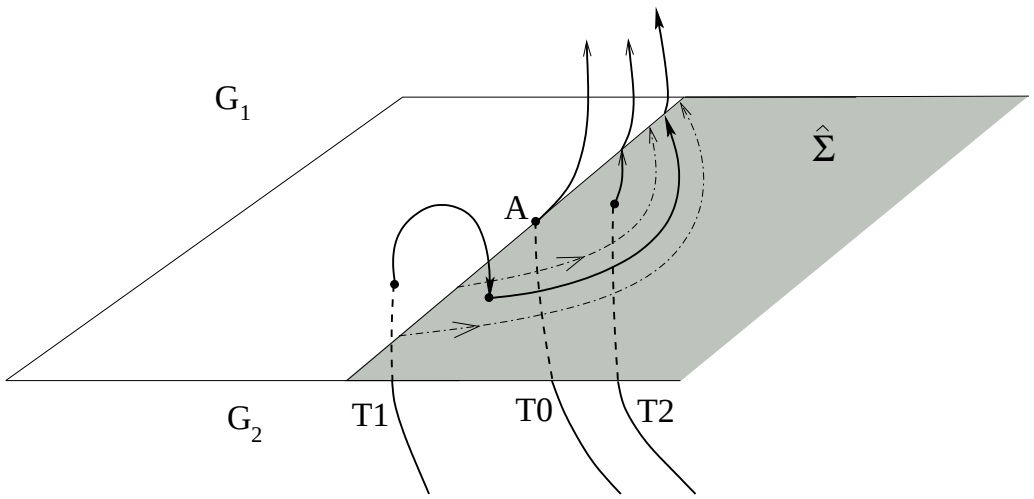

Figure 4: Segment of a trajectory undergoing degenerate sliding bifurcation Case I. At the bifurcation point, the trajectory crosses the switching manifold at the codimension two node denoted by the letter A in Fig. 4. Dashed curves denote projection of the vector field onto the switching manifold Σ. The local maximum of the vector field is clearly visible.

4.1.1 Unfolding in parameter space

As will be detailed later in Sec. 5, these features of the local phase space portrait about the codimension-two point translate into the local unfolding in parameter space depicted in Fig. 5. Here we see that three codimension-1 boundaries in parameter space associated to three different codimension-1 sliding bifurcations meet at the codimension-two point. Schematic orbit diagrams are reported in the figure to show the orbit topology on each of the boundaries and how it changes when different boundaries are crossed. It will be proved (see Sec. 5 for further details) that the three boundaries merge smoothly up to second-order.

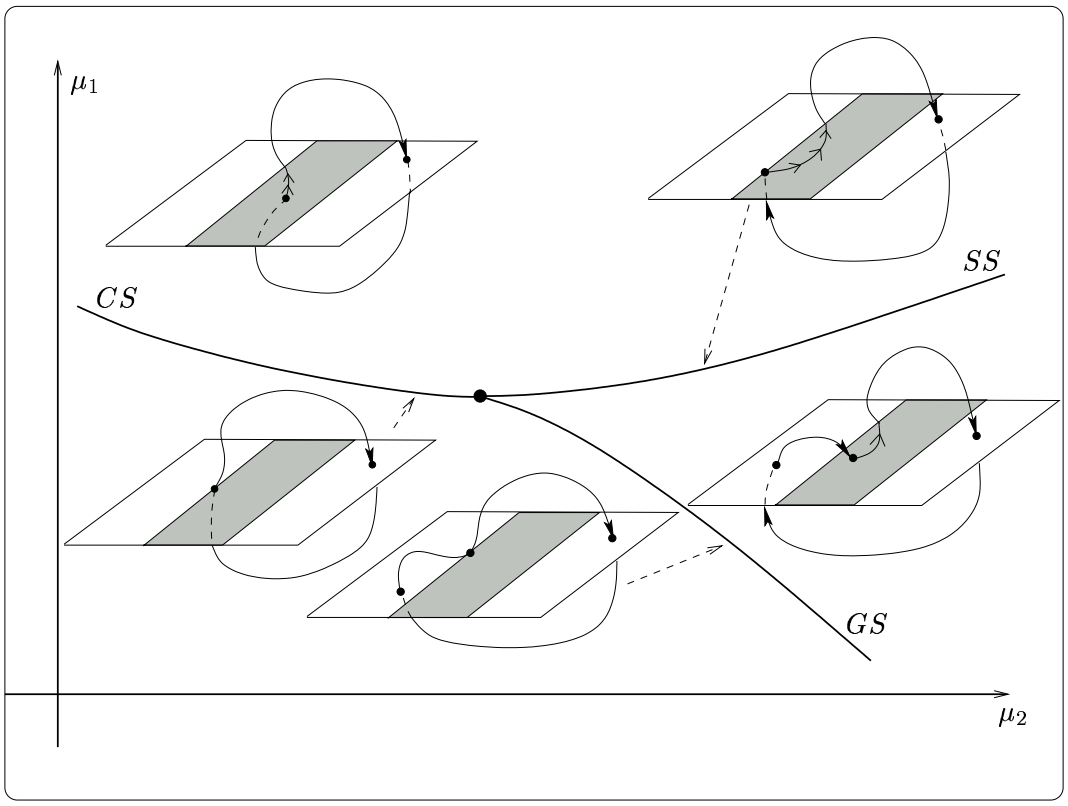

Figure 5: Qualitatively different types of trajectories around the codimension-2 bifurcation point

Note that the fact that three codimension-one boundaries are found to merge at the degenerate point does not contradict the codimension-2 nature of the bifurcation under investigation. Specifically, two of the three boundaries are characterised by the same analytical conditions that can be associated to different topologies of the local phase-space.

4.2 Case II: degenerate switching-sliding and Case III: degenerate grazing-sliding

Another possibility, as explained earlier in Sec. 3, is that conditions (12),(13), (17) and (19) are satisfied. In this case, the negative sign of the additional condition (19) implies that the trajectory exhibits a local minimum of the vector field with respect to the boundary $\partial\hat{\Sigma}^-$.

These conditions can be actually associated to two alternative local phase space portraits. Specifically, as shown in Fig. 6 and Fig. 7, there are two possible codimension-two scenarios associated to the same analytical conditions. They differ with respect to the nature of the incoming bifurcating trajectory. Namely, point A in Fig. 6 is reached by a trajectory generated by flow Φ_2 in region G_2 (case II), while in Fig. 7 the same point is associated to an incoming trajectory generated by flow Φ_1 in region G_1 (case III). Notwithstanding these differences, the character of the outcoming flows remains the same.

Despite sharing the same analytical condition, the difference between the two cases becomes clearer when the local unfolding in parameter space is considered.

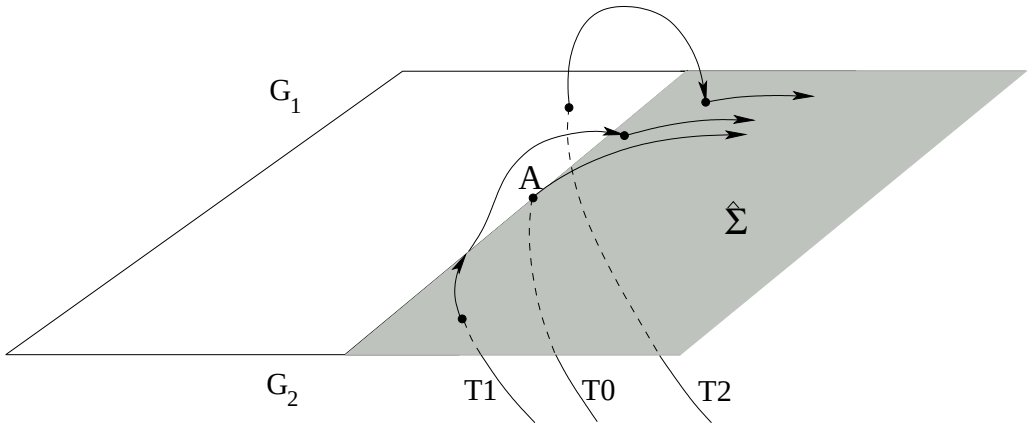

Figure 6: Segment of a trajectory undergoing degenerate codimension-2 sliding bifurcation scenario Case II.

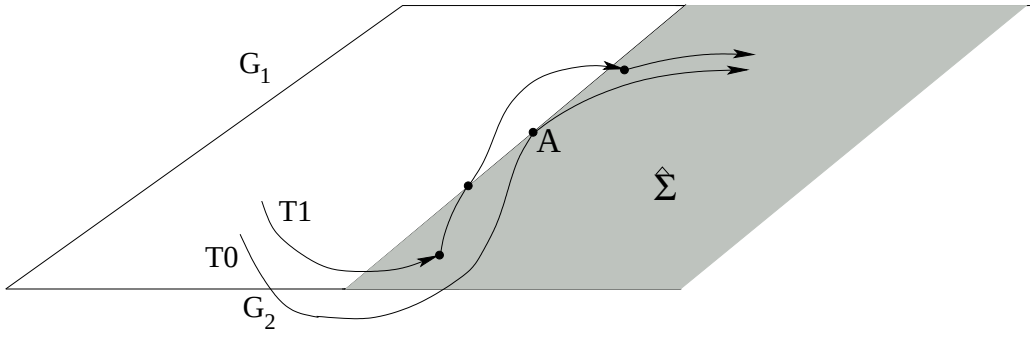

Figure 7: Segment of a trajectory undergoing degenerate sliding bifurcations: Case III

4.2.1 Case II: Unfolding in parameter space

Different local perturbations away from the codimension-two bifurcation point will lead to different trajectories. The resulting behaviour can be unfolded again in parameter space in terms of boundaries associated to codimension-1 sliding bifurcations. In particular, perturbations applied around the bifurcation point result in either classical codimension-1 switching sliding bifurcation scenario or in switching, or adding sliding behaviour (see Fig. 6).

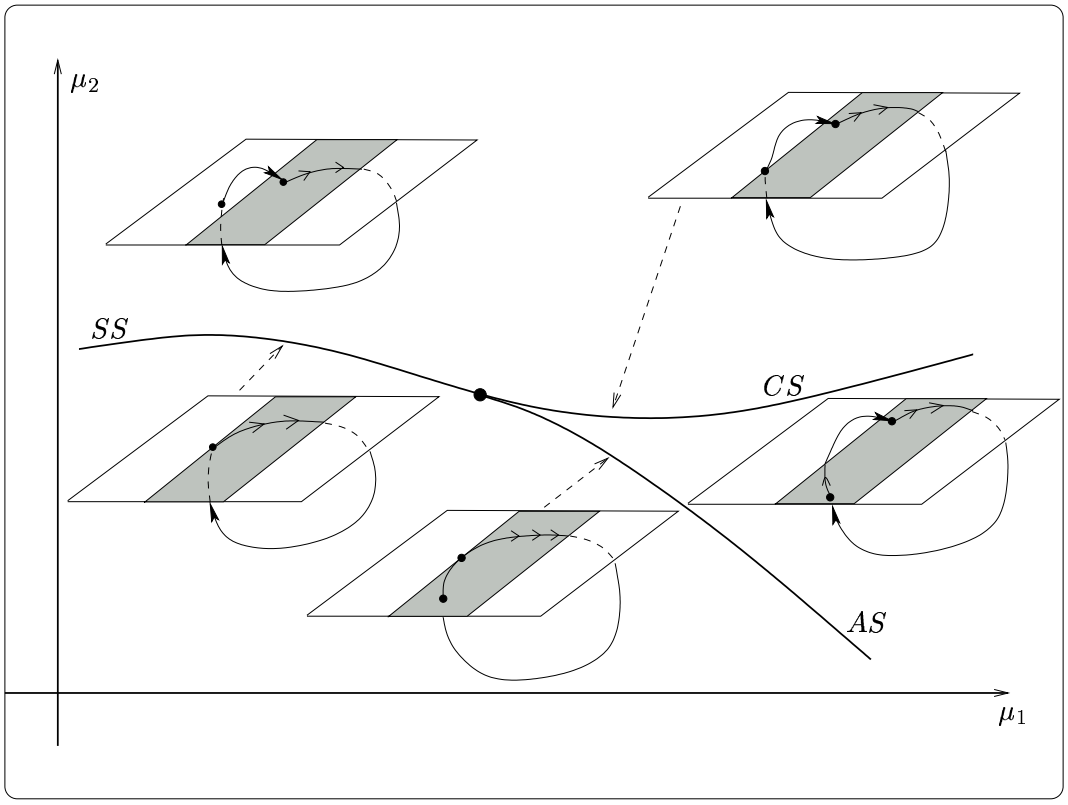

Figure 8: Qualitatively different types of trajectories around the codimension-2 bifurcation point

This is associated to the local unfolding in parameter space shown in Fig. 8. Three boundaries associated to codimension-one sliding bifurcations (sliding-crossing, sliding-switching and sliding-adding) meet at the codimension-two node. Our analysis shows that at the merging point the three boundaries meet smoothly up to quadratic-order.

4.2.2 Case III: Unfolding in parameter space

Perturbations applied around the codimension-2 node will lead to the birth of two branches of codimension-1 sliding bifurcations namely to grazing-sliding and adding sliding bifurcation scenarios (see Fig. 7). The local unfolding in parameter space is depicted in Fig. 9. Note that in this case the two branches merge nonsmoothly at the codimension-two point.

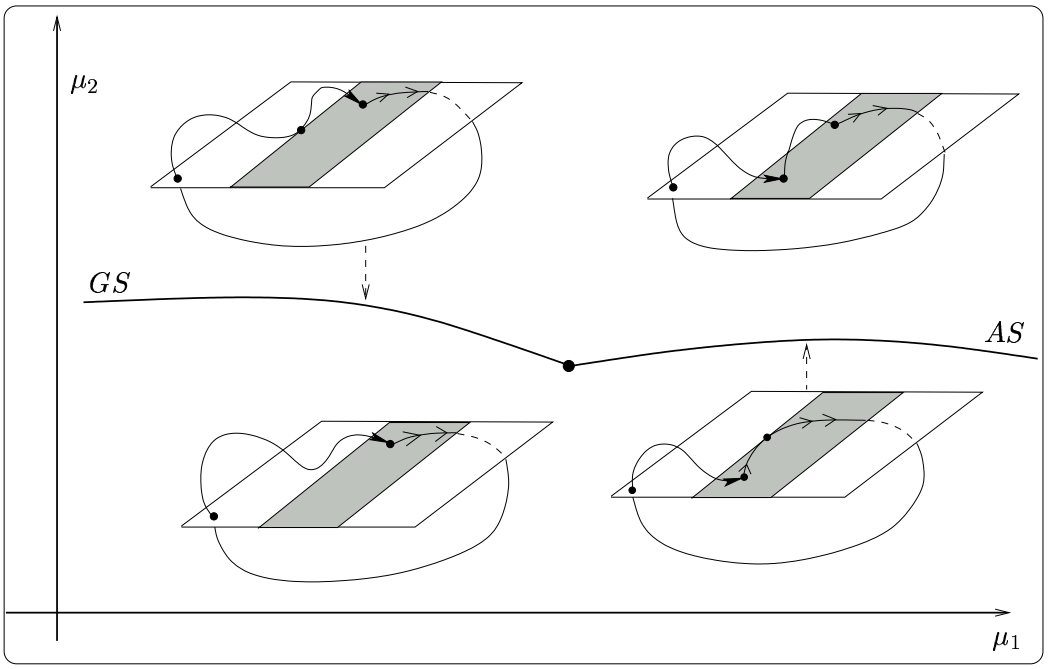

Figure 9: Qualitatively different types of trajectories around the codimension-2 bifurcation point

4.3 Case IV

Now, we shall consider the final case of degenerate codimension-2 sliding bifurcations. This case is brought about by the violation of the nondegeneracy condition (19). This yields that the local minimum of the vector field with respect to the boundary of the sliding region, characterising the previous bifurcation scenarios, changes into a turning point.

The phase portrait associated to these conditions, thus, becomes the one depicted in Fig. 10. Note, that the bifurcating trajectory must approach A from within the sliding set as assumed in Sec. 3 otherwise conditions (12), (13), (17), (20) and (21) describing the bifurcation would imply a codimension-3 event.

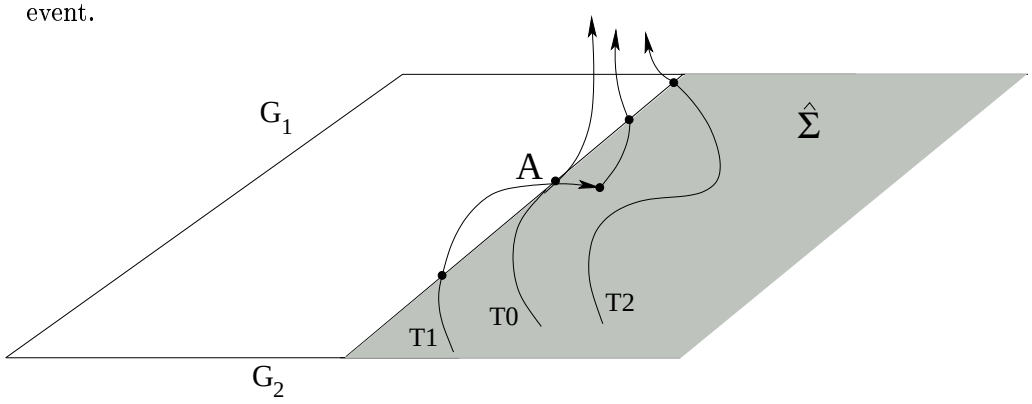

Figure 10: Segment of a trajectory undergoing degenerate sliding bifurcations: Case IV

4.3.1 Unfolding in parameter space

The vector field has locally a cubic character with respect to the bifurcation boundary $\partial\hat{\Sigma}^{-}$. Small perturbations applied to the bifurcating trajectory will result into the local unfolding shown in Fig. 11 Here, at the codimension-2 node, we observe the branching of two boundaries associated to different codimension-1 sliding bifurcations; namely adding-sliding and grazing-sliding (similarly to what described for Case III).

We shall now explain in more details how the results presented in this section were obtained by discussing Case I as a representative example. All the other scenarios were investigated in a likewise manner (the derivation is not reported here for the sake of brevity).

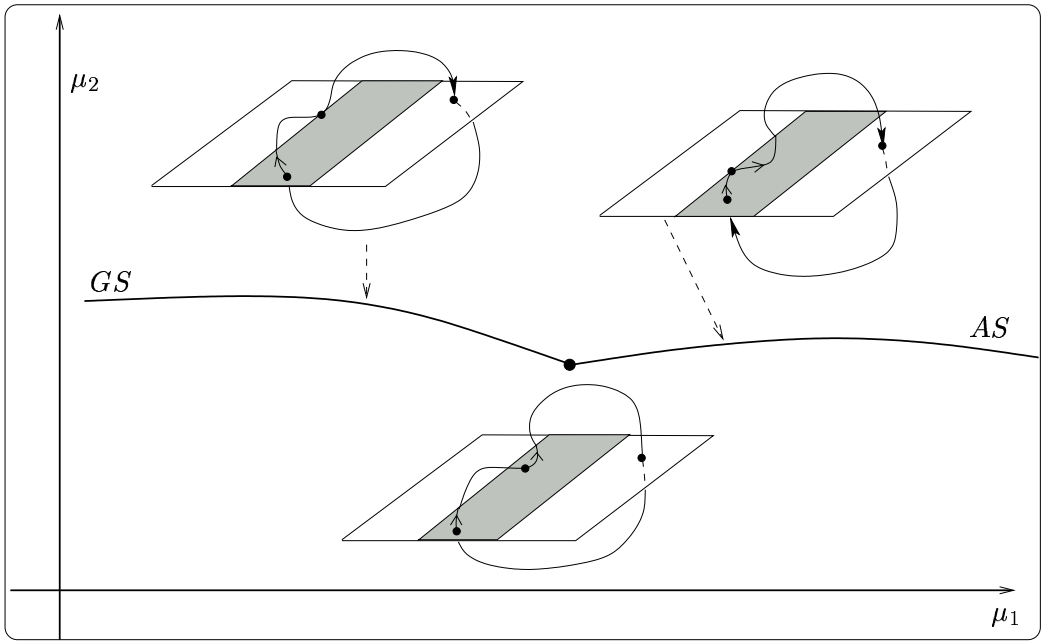

Figure 11: Qualitatively different types of trajectories around the codimension-2 bifurcation point

5 Analysis of degenerate sliding-crossing

To perform a proper unfolding of a codimension-2 degenerate sliding bifurcation point we need to (i) determine local phase portraits about the bifurcation point of interest; (ii) identify the boundaries in parameter space associated to different codimension-one bifurcations branching out of the codimension-two node.

In what follows we will detail the derivation for Case I. All other cases can be treated in a similar manner.

5.1 Local Phase-Space Portrait

Let us focus our attention on Fig. 12. In the figure we schematically sketch the phase space topology locally to the codimension-2 bifurcation node. As discussed in Sec. 4, perturbations about the bifurcation point will lead to three different types of trajectories. We can therefore divide the switching manifold Σ into three regions denoted by R_1, R_2 and R_3 so that:

- Trajectories starting from region R_1 leave the switching manifold towards region G_1 (see trajectory T0 in Fig. 12);
- trajectories starting from region R_2 still leave the switching surface towards G_1 but, after some finite time, will hit the switching manifold again within the sliding region $\hat{\Sigma}$. They then evolve according to the sliding flow until crossing the boundary $\partial\hat{\Sigma}^-$, where they finally leave the switching manifold (see trajectory T1 in Fig. 12);
- trajectories rooted in Region R_3 will evolve according to the sliding flow until $\partial\hat{\Sigma}^-$ is reached. Then, they will leave the switching manifold towards G_1.

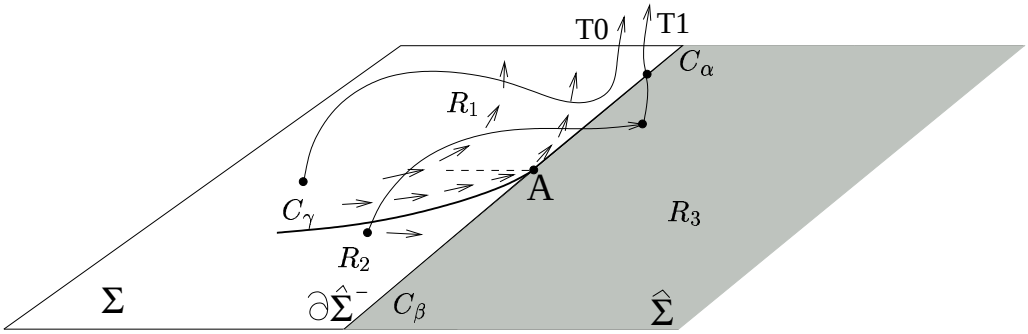

Figure 12: Phase space topology around the codimension-2

To characterise the codimension-two node, we now need to obtain analytical expressions of the boundaries in phase space between these three regions.

Let us first assume that point A is placed at the origin in an appropriately defined set of local coordinates. Obviously, the boundary of the sliding region $\partial\hat{\Sigma}$ is by definition also the boundary between R_3 and $R_1 \cup R_2$.

We know that at the point A the vector field governing the system dynamics is tangential to the boundary and has a local maximum as implied by conditions (17) and (18). Therefore, the quantity $\langle \nabla H, \frac{\partial F_1}{\partial x} F_1 \rangle$ evaluated for $x \in \partial\hat{\Sigma}^-$ must change sign when x is varied past A along $\partial\hat{\Sigma}$. We define:

$$C_\alpha := \{x \in \partial\hat{\Sigma}^- : \langle \nabla H, \frac{\partial F_1}{\partial x} F_1 \rangle > 0\}. \tag{22}$$

and

$$C_\beta := \{x \in \partial\hat{\Sigma}^- : \langle \nabla H, \frac{\partial F_1}{\partial x} F_1 \rangle < 0\}. \tag{23}$$

Now, we need to define the boundary between regions R_1 and R_2 and determine the bifurcation scenario which is observed when this boundary is crossed. It has been mentioned that trajectories starting from region R_1 leave the switching surface whereas trajectories starting from region R_2 return to the switching manifold crossing it within the sliding region. Then, after reaching $\partial\hat{\Sigma}^-$ they leave the switching surface.

Therefore, points belonging to the boundary between regions R_1 and R_2 (denoted by C_γ in Fig. 12) must be associated to trajectories which just graze the boundary of the sliding region (see Fig. 13). In order for this to occur, these trajectories must evolve within region G_1 until hitting tangentially $\partial\hat{\Sigma}$,

i.e. at the point of tangency the vector field must satisfy conditions associated to a grazing-sliding trajectory.

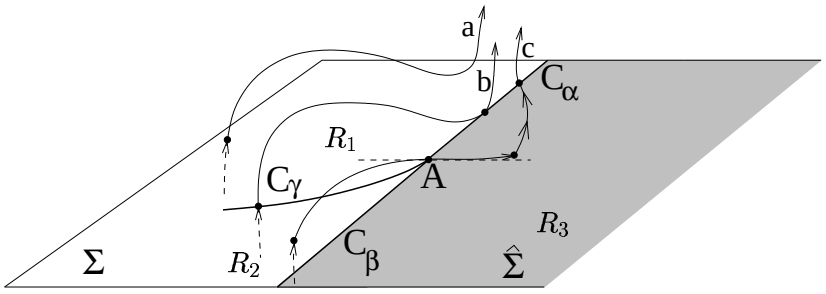

Figure 13: Codimension-1 grazing-sliding bifurcations unfolded from the codimension-2 node

As these conditions can only be satisfied along C_α, it is therefore possible to deduce that C_γ is the inverse image of C_α under the action of flow Φ_1. Thus, we can define C_γ as:

$$C_\gamma := \{x \in \Sigma : C_\alpha \xrightarrow{\Phi_1^{-1}} \Sigma\}, \tag{24}$$

where Φ_1^{-1} refers to the inverse flow governing the dynamics in subspace G_1.

5.2 Analytical Derivation of C_γ

We can derive an analytical approximation of the boundary C_γ expanding the flow Φ_1 as a Taylor series about the codimension-two point, assuming evolution in reverse time. We proceed as follows:

- we expand flow Φ_1 originated from C_α in the close neighbourhood of the point A;
- we derive an approximate expression for the time, say δ, which is required to hit the switching manifold Σ as a function of initial perturbation $\varepsilon\tau_0$ along C_α;
- we then obtain an approximate expression for C_γ;
- finally, we explore how smoothly C_γ joins with C_α.

Expanding the flow as a Taylor series, we can approximate the first intersection, $\bar{x}$, of the trajectory with Σ in reverse time as:

$$\begin{aligned}\bar{x} = \Phi_1(\varepsilon\tau, -\delta) = \varepsilon\tau - F_1\delta + a_1\delta^2 - b_1\varepsilon\tau\delta + \\ -c_1\delta^3 - d_1(\varepsilon\tau)^2\delta + e_1\varepsilon\tau\delta^2 + \mathcal{O}(\varepsilon^4).\end{aligned} \tag{25}$$

Coefficients a_1, b_1, c_1, d_1, e_1 are coefficients of Taylor series expansion and can be found in the appendix. For our purpose it is sufficient to obtain an expression for $\bar{x}$ up to the third order. Since $\langle \nabla H, \bar{x} \rangle = 0$ we then get:

$$\begin{aligned}\langle \nabla H, \bar{x} \rangle \approx \varepsilon\tau_{0H} - F_{1H}\delta + a_{1H}\delta^2 - \varepsilon(b_1\tau_0)_H\delta + \\ -c_{1H}\delta^3 - (d_1\tau_0^2)_H\varepsilon^2\delta + (e_1\tau_0)_H\varepsilon\delta^2 + \mathcal{O}(\varepsilon^4) = 0\end{aligned} \tag{26}$$

where subscript H denotes dot products with the vector ∇H. The first four terms on the right hand side in (26) can be easily shown to vanish. Moreover, due to the fact that both Σ and $\partial\hat{\Sigma}^-$ are flat manifolds, $(d_1\tau_0^2)_H$ is equal

to nought (see [11] for further details). Therefore, we obtain that δ can be expressed as:

$$\delta = \gamma_1 \varepsilon + \gamma_2 \varepsilon^2 + \gamma_3 \varepsilon^3, \tag{27}$$

with

$$\gamma_1 = \frac{\langle \nabla H, e_1 \tau_0 \rangle}{\langle \nabla H, c_1 \rangle}. \tag{28}$$

Substituting the appropriate expressions for c_1 and e_1, we can further evaluate γ_1 as:

$$\gamma_1 = 3 \frac{\langle \nabla H, \left(\frac{\partial F_1}{\partial x} \right)^2 \tau_0 \rangle}{\langle \nabla H, \left(\frac{\partial F_1}{\partial x} \right)^2 F_1 \rangle}. \tag{29}$$

For the sake of brevity we do not present expressions for γ_2 and γ_3. In the next step we substitute (27) into (25) and collect terms at subsequent powers of ε. Thus, we get:

$$\bar{x} = \varepsilon(\tau_0 - \gamma_1 F_1) + \varepsilon^2(-\gamma_2 F_1 + \gamma_1^2 a_1 - \gamma_1 b_1 \tau_0) + \mathcal{O}(\varepsilon^3). \tag{30}$$

Expression (30) is the local approximation of C_γ.

As mentioned at the beginning of this section we want to determine the way in which C_α joins with C_γ (as this allows to make plausible predictions to the nature of different bifurcations around the codimension-2 point). To this aim we need to monitor one component of vector $\bar{x}$ only. Namely, we are interested in the component of $\bar{x}$ projected onto the normal to $\partial\hat{\Sigma}^-$ (we also assume this vector to be coplanar with Σ). Therefore, we apply ∇H_u to $\bar{x}$. [2] Thus, we get:

$$\langle \nabla H_u, \bar{x} \rangle \approx \varepsilon \langle \nabla H_u, (\tau_0 - \gamma_1 F_1) \rangle + \varepsilon^2 \langle \nabla H_u, (-\gamma_2 F_1 + \gamma_1^2 a_1 - \gamma_1 b_1 \tau_0) \rangle. \tag{31}$$

It is trivial to show that both two terms of (31) standing at ε vanish, similarly the first term standing at ε^2. Thus, we can write $\langle \nabla H_u, \bar{x} \rangle$ to leading order as:

$$\begin{aligned} \langle \nabla H_u, \bar{x} \rangle \quad \approx \quad & \varepsilon^2 \left(\frac{9}{2} \langle \nabla H_u, \frac{\partial F_1}{\partial x} F_1 \rangle \frac{\langle \nabla H, \left(\frac{\partial F_1}{\partial x} \right)^2 \tau_0 \rangle^2}{\langle \nabla H, \left(\frac{\partial F_1}{\partial x} \right)^2 F_1 \rangle^2} \right. \\ - \quad & \left. 3 \langle \nabla H_u, \frac{\partial F_1}{\partial x} \tau_0 \rangle \frac{\langle \nabla H, \left(\frac{\partial F_1}{\partial x} \right)^2 \tau_0 \rangle}{\langle \nabla H, \left(\frac{\partial F_1}{\partial x} \right)^2 F_1 \rangle} \right). \end{aligned} \tag{32}$$

We can further simplify the equation above through appropriate algebraic manipulations (omitted here for the sake of brevity). Thus, finally, we get:

$$\langle \nabla H_u, \bar{x} \rangle \approx -\varepsilon^2 \frac{3}{\langle \nabla H, F_2 \rangle} \frac{\langle \nabla H, \left(\frac{\partial F_1}{\partial x} \right)^2 \tau_0 \rangle^2}{\langle \nabla H, \left(\frac{\partial F_1}{\partial x} \right)^2 F_1 \rangle}. \tag{33}$$

[2] Note that ∇H_u does not necessarily need to be coplanar with Σ. Therefore, to get the appropriate quantitative description we need to project ∇H_u onto Σ. Then, the obtained vector needs to be normalised. In this way we can obtain orthonormal to $\partial\hat{\Sigma}^-$ coplanar with Σ. These operations alter the vector ∇H_u, which is applied to $\bar{x}$ but these are purely algebraic manipulations which generically do not change the leading order approximation of ([here ref])

Therefore, the component of $\bar{x}$ along the normal to $\partial\hat{\Sigma}$ at the codimension-two node scales quadratically with the initial perturbation $\varepsilon\tau_0$. Thus, C_γ merges smoothly with C_α at the bifurcation point.

5.3 Classification of the dynamics across C_α, C_β and C_γ

Having explained the phase space topology locally to the codimension-2 node, we now give a general description of the normal form map which captures the essential dynamics of the system around the codimension-2 node. In so doing we make use the concept of zero-time discontinuity mapping (or ZDM) presented in [2, 5]. The normal form (which is derived in the Appendix), in the current case captures the influence of an additional sliding segment of a trajectory born in the bifurcation around the codimension-2 node. It consists of two distinct expressions. We can write this map in the following form:

$$D(x) = \begin{cases} x + M\mu + N\nu \quad \text{when} \quad x \in R_1, \\ x + D\langle C, x\rangle^{3/2} + \mathcal{O}(\varepsilon^2) + M\mu + N\nu \quad \text{when} \quad x \in R_3, \end{cases} \tag{34}$$

where C is some row vector and D, M, N are some column matrices. For the detailed and qualitative description of the normal form derivation see Appendix. Note that, when region R_2 is reached we need first to evaluate the trajectory using flow Φ_1 which is the "natural" flow onto which Φ_2 switches after reaching Σ (see Appendix for details) and then apply the ZDM.

Clearly, from our heuristic description of the phase space topology around the codimension-2 node and the normal form map (34) we can infer much information about the dynamics of a bifurcating limit cycle. As shown in [9] the discontinuity type which is found in the ZDM describing a particular bifurcation scenario, generically characterises the global Poincaré map describing behaviour of a bifurcating limit cycle. The normal form map which captures the local dynamics is therefore found to be smooth (at least C^1 differentiable) across the different bifurcation boundaries.

We can therefore conclude that in a neighborhood of the degenerate codimension-2 node, the bifurcating limit cycle preserves its stability properties and period under parameter perturbations. Depending upon which boundary around the codimension-2 node is crossed the perturbed trajectory will acquire a different number of additional segments. These observations will be important to unfold the codimension-two event in parameter space.

5.4 Unfolding in Parameter Space

It is now important to evaluate how the phase-space boundaries C_α, C_β and C_γ are mapped to corresponding bifurcation boundaries in parameter space. To address this question, we start by noting that, as discussed above, perturbed trajectories about the codimension-two node persist. Thus, using the normal form map presented above, a local map can be constructed from the switching manifold back to itself such that its fixed points are associated to corresponding limit cycles in phase space. The origin of this map will correspond to the bifurcating limit cycle undergoing the codimension-2 event discussed here.

As highlighted in [5, 3], it is possible to show that such mapping is an affine transformation of the form:

$$\underline{x}_{n+1} = A\underline{x}_n + B\mu \tag{35}$$

where μ is an m–dimensional parameter vector, $\underline{x}_n$ an n–dimensional state vector and A, B correspondingly constant matrices.

In general this map is $(n-1)$-dimensional. Therefore to obtain an unfolding of the codimension-two bifurcation in a two-dimensional parameter plane, we need to consider an appropriate projection of $\underline{x}$ and the curves C_α, C_β and C_γ. In our case, to obtain this two dimensional representation we first project C_α, C_γ and C_β onto the plane spanned by the normal to $\partial\hat{\Sigma}^-$ and the vector tangent to $\partial\hat{\Sigma}^-$. (This plane is such that the smoothness property of the boundaries at the codimension-two point are preserved.)

The images of C_α, C_γ and C_β in parameter space are then obtained by considering the set of parameter perturbations which make the fixed point at the origin move along C_α, C_γ and C_β respectively. We define such boundaries as follows:

$$B_{GS} := \{\hat{\mu} \in R^2 : x^* \in C_\gamma\} \tag{36}$$

$$B_{SS} := \{\hat{\mu} \in R^2 : x^* \in C_\beta\} \tag{37}$$

$$B_{CS} := \{\hat{\mu} \in R^2 : x^* \in C_\alpha\} \tag{38}$$

where x^* is the fixed point of map (35) with $\mu = \hat{\mu}$, i.e.

$$\underline{x}^* = A\underline{x}^* + B\hat{\mu}. \tag{39}$$

From (35) it can be inferred that the qualitative character of the bifurcation boundaries has the same features as these of C_α, C_γ, and C_β curves. Thus, B_{GS}, B_{SS} and B_{CS} are smooth curves in parameter space (as depicted in Fig. 5) originating from the codimension-two node. Moreover, B_{GS} and B_{CS} merge smoothly at this point. This is an important result for the development of continuation techniques for sliding bifurcations. It provides us with essential information of branching scenarios encountered when codimension-1 sliding bifurcations are traced and become degenerate.

5.5 Example

We construct a simple example of a system which captures the features of the phase-space locally to the codimension-two node to illustrate and confirm our theoretical derivations. Let us consider a system of the form:

$$F_1 = \begin{pmatrix} -x_2 \\ x_3 \\ -1 \end{pmatrix}, \quad F_s = \begin{pmatrix} 0 \\ x_3 \\ -1 \end{pmatrix}, \quad F_2 = \begin{pmatrix} 2 \\ 0 \\ 0 \end{pmatrix}, \tag{40}$$

where F_s is the vector field describing the sliding flow, F_1 describes the vector field in the subspace G_1 defined as $\{x \in \mathbb{R}^3 : x_1 > 0\}$ and F_2 the vector field in subspace G_2 defined as $\{x \in \mathbb{R}^3 : x_1 < 0\}$. Note that $x_1 = 0$ defines the switching manifold Σ and $x_2 = 0$ defines the boundary of the sliding region $\partial\hat{\Sigma}^-$. The bifurcation point, say A, lies at the origin and the sliding region is entered if $x_2 > 0$ and $x_1 = 0$. Thus, the set of points such that $x_2 < 0$ and $x_1 = 0$ lie outside of the sliding region.

Such a simple system captures the dynamics expected in a neighborhood of a degenerate crossing-sliding bifurcation (case I) as it can be easily verified that the set of analytical conditions (12), (13), (17) and (18) are satisfied.

Moreover, in this case we have:

$$C_\alpha := \{x \in \partial\hat{\Sigma}^- : x_3 \leq 0\} \tag{41}$$

. To find an analytical approximation for C_γ we consider the following initial conditions lying on C_α:

$$x_{10} = 0, \quad x_{20} = 0, \quad x_{30} = \tau \quad \text{for} \quad \tau < 0. \tag{42}$$

Solving the set of ODEs governing the flow Φ_1 (Eq. 40) yields:

$$x_1 = x_{10} - x_{20}t - x_{30}t^2\frac{1}{2} + \frac{1}{6}t^3 \tag{43}$$

$$x_2 = x_{20} + x_{30}t - \frac{1}{2}t^2 \tag{44}$$

$$x_3 = x_{30} - t. \tag{45}$$

We seek to find some time t such that $x_1 = 0$. Thus, solving (43) yields $t = 3\tau$. Since, we demand τ to be negative this solution agrees with our assumption that we are seeking solutions in reverse time. Then, parametrising x_2 and x_3 by τ yields:

$$x_2 = -\frac{3}{2}\tau^2, \tag{46}$$

$$x_3 = -2\tau. \tag{47}$$

Thus, combining (46) and (47) we get:

$$C_\gamma := \{x \in \Sigma : x_2 + \frac{3}{8}x_3^2 = 0, \quad x_3 \geq 0\}. \tag{48}$$

Obviously, (48) is differentiable at the origin. Thus, C_α and C_γ join at the codimension-2 node in a smooth fashion.

It is worth mentioning here that (46) and (47) can be also obtained by the straightforward application of equation (31). We note, that:

$$\nabla H_u = \begin{bmatrix} 0 & 1 & 0 \end{bmatrix}, \tag{49}$$

which is coplanar with Σ and of unit length. Therefore formula (31) can be directly applied to our system and compared with (46)-(47). It is straightforward to show that the denominator of (31) is equal to 2. Finally, since vector $\varepsilon\tau_0$ can be written as $\begin{bmatrix} 0 & 0 & \varepsilon\tau_0 \end{bmatrix}$, we get:

$$\langle \nabla H_u, \bar{x} \rangle = -\frac{3}{2}(\varepsilon\tau_0)^2 \tag{50}$$

where $\bar{x}$ denotes an approximate expression of the vector describing x_2 and x_3 on C_γ. This agrees with the expressions found earlier.

We can also check the linear term of (30) which as expected for our example yields:

$$\begin{bmatrix} 0 & 0 & -2\varepsilon\tau_0 \end{bmatrix}. \tag{51}$$

6 An application: the friction oscillator

Let us consider a dry-friction oscillator with external forcing, which in the non-dimensionalised form can be expressed as:

$$\ddot{x} + x = \sin(\omega t) - F\mathrm{sgn}(\dot{x}), \tag{52}$$

where x is the position of the oscillating mass, $\dot{x}$ its velocity while ω and F represent the frequency of the forcing term and the amplitude of the friction characteristic respectively. The system has been extensively studied in [12] but never from the standpoint of bifurcation theory of piecewise smooth systems (PWS). The existence of some of the codimension-2 nodes found by Feigin in [12] have been verified numerically. In particular, the numerical exploration of the ω,

F parameter space led to the detection of a degenerate codimension-2 crossing-sliding bifurcation. An orbit undergoing such a bifurcation has been found at the parameter values: $\omega^* = \frac{1}{2}$, $F^* = \frac{1}{3}$ with the degenerate sliding-crossing occurring at $x = -1.3399$, $\dot{x} = 0$, $\omega t = \frac{3}{2}\pi$. The period of the oscillations is given by $T = 2\frac{\pi}{\omega^*} = 4\pi$. The bifurcating orbit is depicted in the 3-dimensional phase space in Fig. 14. Before we examine the phase space locally around

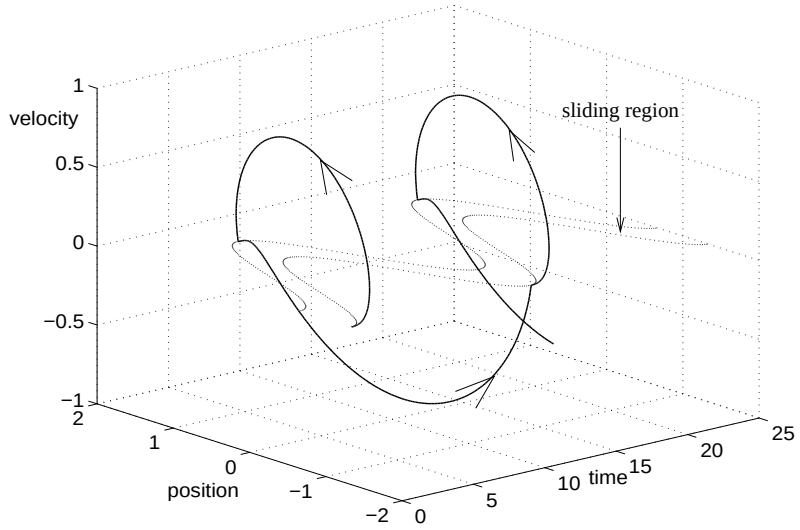

Figure 14: Bifurcating trajectory in 3-dimensional phase space

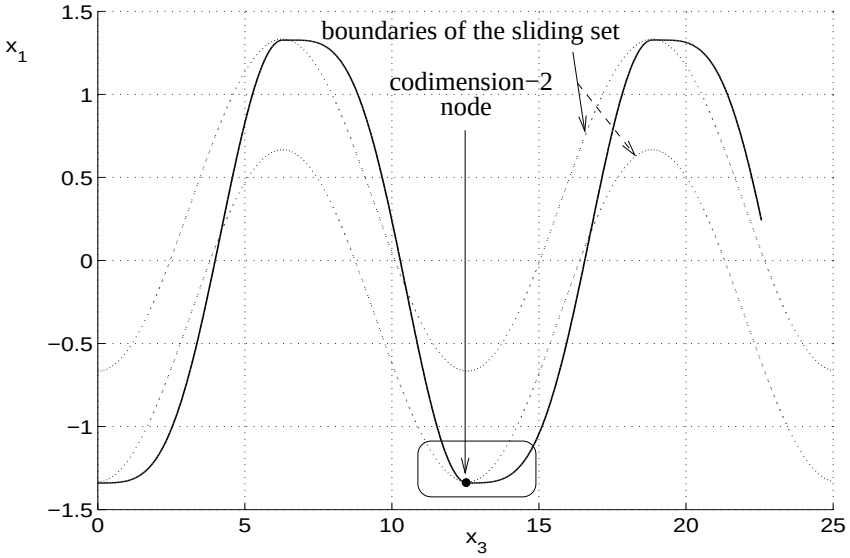

Figure 15: Projection of the bifurcating trajectory onto time-space coordinates. x_1 denotes position and x_3 the time coordinate.

the codimension-2 node let us first check if the set of analytical conditions determining the bifurcation is satisfied.

6.1 System representation

To proceed with our analysis, let us first express the system under consideration as a set of first order autonomous ODEs. Setting the variables $x_1 = x$, $x_2 = \dot{x}$ and $\omega t = \tau$, (52) becomes:

$$\dot{\underline{x}} = \begin{pmatrix} x_2 \\ -x_1 + \sin(\tau) - F\mathrm{sgn}(x_2) \\ \omega \end{pmatrix}. \tag{53}$$

The system trajectory evolves smoothly in two subspaces defined by the sign of the scalar function $H(\underline{x}) = x_2$. We can write (53) as:

$$\dot{x} = \begin{cases} F_1(\underline{x}) & \text{if} \quad H(\underline{x}) > 0 \\ F_2(\underline{x}) & \text{if} \quad H(\underline{x}) < 0 \end{cases} \tag{54}$$

where

$$F_1 = \begin{pmatrix} x_2 \\ -x_1 + \sin(\tau) - F \\ \omega \end{pmatrix}, \tag{55}$$

$$F_2 = \begin{pmatrix} x_2 \\ -x_1 + \sin(\tau) + F \\ \omega \end{pmatrix}. \tag{56}$$

The switching manifold Σ is defined as:

$$\Sigma := \{\underline{x} \in \mathbb{R}^3 : H(\underline{x}) = x_2 = 0\} \tag{57}$$

with the normal to Σ given by $\nabla H = \begin{bmatrix} 0 & 1 & 0 \end{bmatrix}$. The necessary condition ($\langle \nabla H, F_2 \rangle - \langle \nabla H, F_1 \rangle > 0$), which needs to be satisfied for the sliding region to be simultaneously attracting implies the condition $2F > 0$, which holds since the amplitude of the friction characteristic is positive. Therefore, using Utkin's equivalent control method [20] we can obtain the vector field F_s, which governs the flow within Σ, as:

$$F_s = \begin{pmatrix} x_2, \\ -x_1 + \sin(\tau) + H_u F \\ \omega. \end{pmatrix}. \tag{58}$$

The equivalent control H_u defined by (7) yields:

$$H_u = \frac{x_1}{F} - \frac{1}{F}\sin(\tau). \tag{59}$$

and we can define the sliding region as:

$$\hat{\Sigma} := \{\underline{x} \in \Sigma : -1 \leq H_u(\underline{x}) \leq 1\}, \tag{60}$$

or equivalently:

$$\hat{\Sigma} := \{\underline{x} \in \Sigma : -1 \leq \frac{x_1}{F} - \frac{1}{F}\sin(\tau) \leq 1\}. \tag{61}$$

The boundaries of the sliding region $\hat{\Sigma}$ are:

$$\partial\hat{\Sigma}^- := \{x \in \Sigma : \frac{x_1}{F} - \frac{1}{F}\sin(\tau) = -1\} \tag{62}$$

and

$$\partial\hat{\Sigma}^+ := \{x \in \Sigma : \frac{x_1}{F} - \frac{1}{F}\sin(\tau) = 1\}. \tag{63}$$

6.2 Degenerate crossing sliding

Having represented the system of interest in the appropriate form we are now ready to check if the set of analytical conditions determining the degenerate crossing sliding is satisfied at the bifurcation point. Once, we establish this result we can further numerically analyse the phase space around the codimension-2 node and determine if our numerical findings agree with the discussion presented in Sec. 5.1. Before, checking conditions (12) - (18), we should note that we derived these conditions under the assumption that the boundary of the sliding region is a well-defined and flat manifold (at least up to $\mathcal{O}(4)$). In our case the boundary of the sliding region is well defined but not flat (see Eq. 62). Therefore to check analytical conditions (12)–(18) we need to apply a set of transformations which will flatten the boundary of the sliding region around the bifurcation node. For our purpose it is sufficient to flatten the boundary up to the quadratic order. Therefore, we introduce the following set of coordinate transformations:

$$\bar{x}_1 = x_1 - \tfrac{1}{2}(\tau - \tfrac{3}{2}\pi)^2, \tag{64}$$

$$\bar{x}_2 = x_2, \tag{65}$$

$$\bar{\tau} = \tau. \tag{66}$$

In the new set of coordinates we can write (55) as:

$$\bar{F}_1 = \begin{pmatrix} \bar{x}_2 - (\bar{\tau} - \frac{3}{2}\pi)\omega, \\ -\bar{x}_1 - \frac{1}{2}(\bar{\tau} - \frac{3}{2}\pi)^2 + \sin(\bar{\tau}) - F, \\ \omega \end{pmatrix}. \tag{67}$$

Conditions (12) is trivially satisfied as we lie on the switching manifold Σ at the bifurcation point. Condition (13) is 0 within the numerically accuracy. Condition (17) reads:

$$-\bar{x}_2^*(\bar{\tau}^* - \frac{3}{2}\pi)\omega^* + (-\bar{\tau}^* + \frac{3}{2}\pi + \cos(\bar{\tau}^*))\omega^* \tag{68}$$

which is identically 0. Finally, we need to verify condition (18) which yields:

$$\bar{x}_1^* + \frac{1}{2}(\bar{\tau}^* - \frac{3}{2}\pi)^2 - \sin(\bar{\tau}^*) + F + \omega^{*2} = -0.006 + \frac{1}{4} > 0. \tag{69}$$

6.2.1 Phase space topology around the codimension-2 node

Having successfully verified that the codimension-2 node is indeed a degenerate crossing sliding point we will now present our numerical results describing the phase space topology around the node.

From our analytical predictions three different regions R_1, R_2 and R_3 associated to different system qualitative behaviour can be identified locally to the bifurcation point. The boundaries between R_3 and $R_1 \cup R_2$ coincide with the boundary of the sliding region (see Fig. 16). The boundary between R_1 and R_2 was obtained by reverse numerical integration of points lying on C_α. It is clearly seen that C_α and C_γ are found to join smoothly at the bifurcation point as predicted by our analytical derivations.

To confirm the different nature of trajectories rooted in each of the three regions mentioned above, time series of the system evolution with different initial conditions are reported in Fig. 17. Again the numerical simulations agree with what was expected from the analysis.

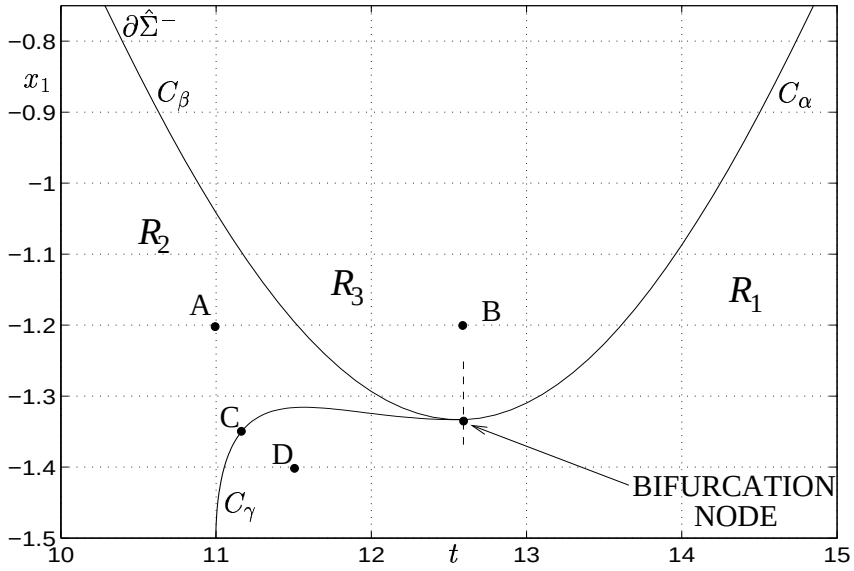

Figure 16: Boundaries in the phase space around the degenerate crossing codimension 2 node

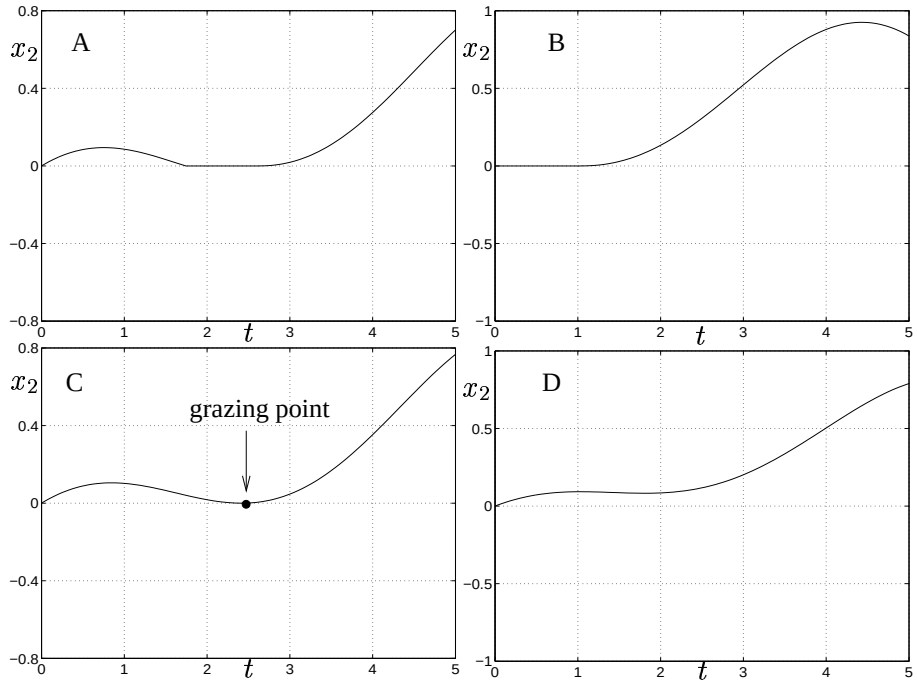

Figure 17: Qualitatively different trajectories around the codimension-2 node starting from regions R_1, R_2 and R_3.Time series representing the velocity coordinate of the trajectories starting in every of the three regions are shown in each of the panels. Each panel is labelled with the letter indicating the starting point in phase space as shown in Fig. 16.

6.2.2 Classification of the dynamics around the codimension-2 node

Now, we can attempt to predict the bifurcation scenario around the codimension-2 node. We first need to determine if the bifurcating limit cycle is an hyperbolic cycle. To this aim we evaluate eigenvalues of the Jacobian matrix, say J of a $T-$time map of the flow built around the periodic point of the bifurcating orbit. In the current case it is sufficient to calculate the eigenvalues of the map obtained by considering the evolution along the half period $\frac{T}{2}$ as the orbit is symmetric.

It is easy to verify that the sought matrix J has the following form:

$$J = \begin{pmatrix} \cos(T/2) & \sin(T/2) \\ -\sin(T/2) & \cos(T/2) \end{pmatrix} \tag{70}$$

Note, that at the bifurcation node $\omega^* = \frac{1}{2}$ and $\frac{T}{2} = \frac{\pi}{\omega}$ therefore the bifurcating orbit is non-hyperbolic. Thus, it would seem that we are dealing with a codimension-3 event that cannot be solely determined based on our previous discussion.

In fact, in the current case we can show that the bifurcation scenario is indeed a codimension-2 event. Namely, it can be shown that a simple symmetric orbit (e.g. an orbit with no sliding segment of period $T = \frac{2\pi}{\omega}$, crossing the switching manifold twice per period) undergoing a codimension-two degenerate crossing sliding bifurcation must be non-hyperbolic.

Let us assume such an orbit exists. Then, it will cross the switching manifold at the codimension-two point, say $(x_0, 0, \tau_0)$. Solving the system ODEs with initial conditions $(x_0, 0, \tau_0)$, we get:

$$\begin{aligned} x\left(\frac{\pi}{\omega}\right) = \frac{\cos(\frac{\pi}{\omega})F\omega^2 + \cos(\frac{\pi}{\omega})x_0\omega^2 - F\omega^2 + \sin(\frac{\pi}{\omega})\omega\cos(\tau_0) + F}{(-1+\omega^2)} + \\ \frac{+\cos(\frac{\pi}{\omega})\sin(\tau_0) - \cos(\frac{\pi}{\omega})F - \cos(\frac{\pi}{\omega})x_0 + \sin(\tau)}{(-1+\omega^2)} \end{aligned} \tag{71}$$

where τ_0 denotes initial phase and x_0 initial position.

From condition (13), we know that the initial point belongs to the boundary $\partial\hat{\Sigma}^-$ which implies $x_0 = -F + \sin(\tau^0)$. Moreover, conditions (17)–(18) require that the initial phase must be equal to $\frac{3\pi}{2}$.

Furthermore noting that $x(\frac{\pi}{\omega}) = -x_0$ and $\dot{x}(\frac{\pi}{\omega}) = 0$ we can write the following set of two equations which need to be satisfied at the degenerate codimension-2 node:

$$\frac{\sin\left(\frac{\pi}{\omega}\right)\omega^2}{-1+\omega^2} = 0, \tag{72}$$

$$F = \frac{1}{2}\frac{\omega^2(\cos(\frac{\pi}{\omega})+1)}{1-\omega^2}. \tag{73}$$

Thus, we find that the codimension-two bifurcation can only occur for parameter values F^* and ω^* satisfying (72), (73). In particular, for (72) to be non-singular and identically nought we require that $\omega = \frac{1}{n}$ with $n = 2, 3, \ldots,$. As we require friction to be non zero $F \neq 0$, from (73) we can rule out odd integers of n. Therefore, we must have:

$$\omega^* = \frac{1}{2n}, \tag{74}$$

$$F^* = \frac{\omega^{*2}}{1-\omega^{*2}}. \tag{75}$$

Note that in the friction oscillator under investigation, the codimension-two bifurcation was located for $\omega^* = \frac{1}{2}$ and $F^* = \frac{1}{3}$ which clearly satisfy (74) and (75).

It can be clearly seen that for any ω^* satisfying (74), the Jacobian matrix (70) turns out to be singular. This confirms our conjecture that the degenerate crossing-sliding detected in the friction oscillator is a codimension-two event.

We can finally classify the bifurcation scenarios around the codimension-2 node. In particular we are interested in understanding the bifurcation events detected when ω and F are varied in a sufficiently small neighborhood of ω^* and F^*. Note that:

- the stability of a simple orbit is determined by the eigenvalues of the Jacobian (70) which are always within the unit circle for any value of $\omega \neq \omega^*$;
- it can be trivially shown that in this case additional sliding segments cannot destabilise a given orbit;

Therefore, the only effect of varying the parameter about the codimension-two point is to cause the bifurcating orbit to acquire or loose additional segments of trajectory belonging to region G_1 or/and the sliding region $\hat{\Sigma}$. Since, crossing of the codimension-1 sliding bifurcation boundaries around the codimension-2 node cannot change the stability properties of bifurcating orbit this, in turn implies that there are no unstable orbits around the codimension-2 node. Thus, it has been confirmed that in our particular case due to the degenerate crossing sliding we can not observe sudden jumps to different attractors. Crossing of different boundaries forces an orbit to acquire additional segments of the trajectory but the orbit preserves its stability and period. This has been confirmed by our numerical simulations.

7 Conclusions

In this paper, we have discussed codimension-2 sliding bifurcations which can be observed in Filippov type systems due to the violation of the non degeneracy conditions for sliding bifurcations of codimension-1. We have shown that four different codimension-2 sliding bifurcations can be found (see Fig. 3). We discussed the phase space topology and the associated unfolding in parameter space around each of the degenerate bifurcation nodes under consideration. We focused our attention on the degenerate crossing sliding case. Based on the discussion of the phase space topology we showed how three curves of codimension-1 sliding bifurcations join at the codimension-2 node. Since, the bifurcation boundaries form a curve which separates smoothly into two branches at the codimension-2 node we assumed that this scenario should be translated onto the normal form describing the bifurcation. Derivation of the normal form confirmed that the discontinuity can be encountered in the higher order terms of the normal form map, therefore a hyperbolic orbit undergoing this type of sliding bifurcations preserves its stability properties and period when crossing the different bifurcation boundaries around the codimension-2 node. This is a very crucial remark since in the classical grazing sliding case (one of the three boundaries joining in the node is the grazing sliding boundary) the normal form map is PWL which in turn implies that a sudden jump to different attractors is possible. In Sec. 6 we investigated numerically a dry-friction oscillator where degenerate crossing sliding bifurcations has been found. We showed that simple symmetric orbit due to the degenerate crossing sliding bifurcation acquires additional segments but preserves its stability and period thus confirming our

analytical predictions. Here, we should note however that the orbit was non-hyperbolic. We showed that non-hyperbolicity of the orbit is in fact triggered by to the violation of non-degeneracy condition (17).

We anticipate that the results presented in the paper will be particularly relevant for the development of algorithms and routines for the numerical continuation of C-bifurcations in piecewise-smooth systems. Namely, the local unfolding presented here will be useful to design appropriate branching routines to be embedded in an appropriate continuation tool for systems with discontinuities. Future work will be directed towards the development and application of such numerical tools as well as the investigation of other classes of codimension-two phenomena.

Acknowledgements

The authors wish to thank Dr Arne Nordmark, KTH, Sweden and Prof. A.R. Champneys, University of Bristol, U.K., for their insightful comments, remarks and suggestions. In particular, we wish to acknowledge that Sec. 5 and the example presented in Sec. 5.5 were the result of such discussions. The authors gratefully acknowledge support from the EPSRC (Bristol Centre for Applied Nonlinear Mathematics – grant no. GR/R72020) and the European Union (FP5 Project SICONOS IST-2001-37172).

A Appendix. Normal form map of the degenerate crossing-sliding bifurcations

We consider degenerate Case I codimension-2 sliding bifurcation scenario. To derive the ZDM normal form map which captures the dynamics locally to the bifurcation node we need to refer to the concept of the zero time discontinuity mapping (ZDM). In case of sliding bifurcations the ZDM captures the influence of additional segment of a trajectory which is born in the bifurcation (see [11] for details). Therefore, we need to pose a question what is the new segment of a flow which arises around the codimension-2 node when the degenerate Case I sliding bifurcation takes place. Let us refer to Fig. 12. If region R_1 is hit no bifurcation takes place in the system. The evolving trajectory switches between flows ϕ_2 and ϕ_1 at the discontinuity set Σ (ϕ_2 refers to the flow generated by the vector field F_2 governing the dynamics in subspace G_2 and ϕ_1 refers to the vector field F_1 governing the dynamics in subspace G_1 see Sec 1.1). We shall now consider what happens when switchings occur within R_3 or R_2 parts of Σ. If R_3 is encountered we observe the following transition of flows: from ϕ_2 to ϕ_s (ϕ_s governs the sliding dynamics on – see Sec 1.1) and then after the boundary $\partial\hat{\Sigma}^-$ is reached ϕ_s switches to ϕ_1. Finally, if switching occurs within R_2 the trajectory first switches to flow ϕ_1 and then reaches the sliding subset thus evolving within $\hat{\Sigma}$ until reaching the boundary $\partial\hat{\Sigma}^-$. Then, again the trajectory follows ϕ_1. We can describe how the vector fields switch around the codimension-2 node depending on the region where the switching occurs in the symbolic way as:

$$\begin{aligned}
\phi_2 &\longrightarrow \phi_1 \quad \text{region } R_1 \text{ no bifurcation} \\
\phi_2 &\longrightarrow \phi_s \longrightarrow \phi_1 \quad \text{region } R_3, \\
\phi_2 &\longrightarrow \phi_1 \longrightarrow \phi_s \longrightarrow \phi_1 \quad \text{region } R_2.
\end{aligned}$$

Obviously, the additional segment of the flow born in the bifurcation is the sliding segment generated by flow ϕ_s. Thus, we can describe the switchings

around the codimension-2 node using only flows ϕ_2 and ϕ_1 and the ZDM as follows:

$$\begin{aligned}\phi_2 &\longrightarrow \phi_1 \quad \text{region } R_1 \text{ no bifurcation}\\ \phi_2 &\longrightarrow ZDM \longrightarrow \phi_1 \quad \text{region } R_3,\\ \phi_2 &\longrightarrow \phi_1 \longrightarrow ZDM \longrightarrow \phi_1 \quad \text{region } R_2.\end{aligned}$$

Therefore, we need to derive the ZDM map which captures the influence of the sliding flow on the system dynamics locally around the codimension-2 bifurcation node. Let us focus on the case depicted in Fig. 18. The bifurcating trajectory is crossing the switching manifold Σ at the bifurcation point A lying on the boundary $\partial\hat{\Sigma}^-$. In order to derive the ZDM we shall proceed in two

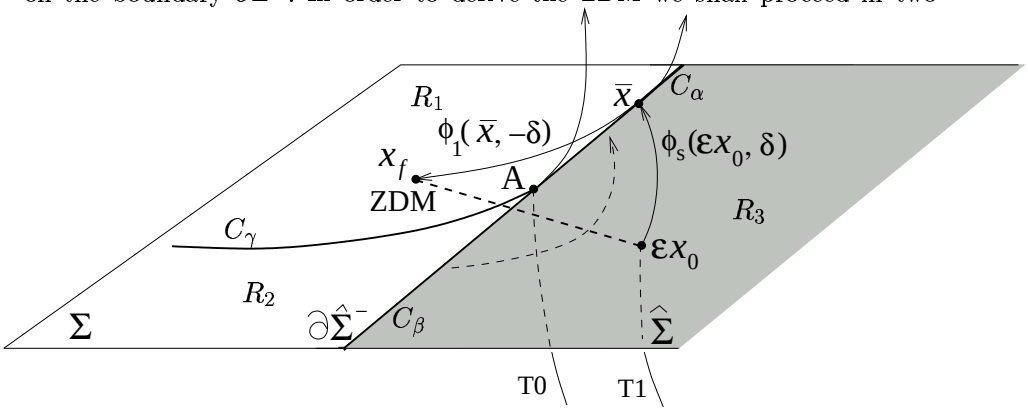

Figure 18: Construction of the ZDM in the degenerate Case I of sliding bifurcations: Mapping D

steps: (i) we evaluate the trajectory from some point, say εx_0 to the point $\hat{x}$ lying at the boundary of the sliding strip using flow ϕ_s; (ii) then we follow ϕ_1 for some time, $-\delta$ until we reach the final point x_f. Therefore, the total time which elapsed to get from εx_0 to x_f is 0. The desired ZDM is a map from εx_0 to x_f (see Fig. 18). To carry out the derivation, we will assume that the vector fields F_1, F_2, F_s are well defined over the entire phase space region of interest. Therefore, we will suppose that the corresponding flows can be expanded as a Taylor series about the bifurcation point $x^* = 0$, $t^* = 0$ as:

$$\begin{aligned}\phi_i(x,t) = x + F_i t + a_i t^2 + b_i x t + c_i t^3 + d_i x^2 t + e_i x t^2 +\\ + f_i t^4 + g_i x^3 t + h_i x^2 t^2 + j_i x t^3 + \mathcal{O}(5),\end{aligned} \tag{1}$$

where $i = 1, s$, $\mathcal{O}(5)$ indicates terms of order equal or higher than five and:

$$\begin{aligned}
&a_i = \frac{1}{2}\frac{\partial F_i}{\partial x}F_i, \quad b_i = \frac{\partial F_i}{\partial x}, \quad c_i = \frac{1}{6}\left(\frac{\partial^2 F_i}{\partial x^2}F_i^2 + \left(\frac{\partial F_i}{\partial x}\right)^2 F_i\right), \quad d_i = \frac{1}{2}\frac{\partial^2 F_i}{\partial x^2},\\
&e_i = \frac{1}{2}\left(\frac{\partial^2 F_i}{\partial x^2}F_i + \left(\frac{\partial F_i}{\partial x}\right)^2\right), \quad f_i = \frac{1}{24}\left[\frac{\partial^3 F_i}{\partial x^3}F_i^3 + \frac{\partial^2 F_i}{\partial x^2}\left(F_i\frac{\partial F_i}{\partial x} + \frac{\partial F_i}{\partial x}F_i\right)F_i +\right.\\
&\left. + \left(\frac{\partial^2 F_i}{\partial x^2}\frac{\partial F_i}{\partial x} + \frac{\partial F_i}{\partial x}\frac{\partial^2 F_i}{\partial x^2}\right)F_i^2 + \left(\frac{\partial F_i}{\partial x}\right)^3 F_i\right], \quad g_i = \frac{1}{6}\frac{\partial^3 F_i}{\partial x^3},\\
&h_i = \frac{1}{4}\left(\frac{\partial^3 F_i}{\partial x^3}F_i + \frac{\partial F_i}{\partial x}\frac{\partial^2 F_i}{\partial x^2}\right),\\
&j_i = \frac{1}{6}\left[\frac{\partial^3 F_i}{\partial x^3}F_i^2 + \frac{\partial^2 F_i}{\partial x^2}\frac{\partial F_i}{\partial x}F_i + 2\frac{\partial^2 F_i}{\partial x^2}F_i\frac{\partial F_i}{\partial x} + \frac{\partial F_i}{\partial x}\frac{\partial^2 F_i}{\partial x^2}F_i + \frac{\partial F_i}{\partial x}^3\right].
\end{aligned} \tag{2}$$

Note that we have used a shorthand notation here for the higher-order derivative terms, for example

$$\frac{\partial^3 F_i}{\partial x^3}x^3 = \sum_{n,m,p=1,2,3} \frac{\partial^3 F_i}{\partial x_n x_m x_p} x_n x_m x_p \ .$$

In what follows, we shall continue to use this shorthand, with care taken to correctly evaluate the derivative tensors when required.

A.1 First step

Let $x_m(t) = \phi_s(0,t)$ be the trajectory which undergoes the degenerate crossing sliding bifurcation. We consider $\varepsilon-$perturbations of $x_m(t)$ of the form:

$$x(t) = \phi_1(\varepsilon x_0, t) \tag{3}$$

for some x_0 which we assume to be such that:

$$\langle \nabla H_u, x_0 \rangle > 0. \tag{4}$$

Condition (4) ensures that, for $\varepsilon > 0$, the trajectory crosses the switching manifold within the sliding region $\hat{\Sigma}$. Firstly, we evaluate flow ϕ_s from some point εx_0 until the trajectory intersects boundary of the the sliding region at some point, say $\bar{x}$. Assume such intersection to take place after some time δ, we have:

$$\begin{aligned} \bar{x} \ &= \ \phi_1(\varepsilon x_0, \delta) \approx \varepsilon x_0 + \delta F_s + \delta^2 a_s + \varepsilon\delta b_s x_0 + \delta^3 c_s + \varepsilon^2\delta d_s x_0^2 + \\ &\quad + \varepsilon\delta^2 e_s x_0 + \delta^4 f_s + \varepsilon^3\delta g_s x_0^3 + \varepsilon^2\delta^2 h_s x_0^2 + \varepsilon\delta^3 j_s x_0. \end{aligned} \tag{5}$$

We wish to define δ to be the time such that $H(\bar{x}) = 0$, which since $H_u(0) = -1$ and $\partial\hat{\Sigma}^-$ is flat, implies:

$$\langle \nabla H_u, \bar{x} \rangle = 0. \tag{6}$$

Using (5) for $\bar{x}$, (6) yields to leading order:

$$\begin{aligned} &\varepsilon x_{0H_u} + \delta F_{sH_u} + \delta^2 a_{sH_u} + \varepsilon\delta(b_s x_0)_{H_u} + \delta^3 c_{sH_u} + \varepsilon^2\delta(d_s x_0^2)_{H_u} + \varepsilon\delta^2(e_s x_0)_{H_u} + \\ &+\delta^4 f_{sH_u} + \varepsilon^3\delta(g_s x_0^3)_{H_u} + \varepsilon^2\delta^2(h_s x_0^2)_{H_u} + \varepsilon\delta^3(j_s x_0)_{H_u} = 0. \end{aligned} \tag{7}$$

At the bifurcation point, we have $\langle \nabla H_u, F_1 \rangle = 0$ (see condition (17) and equation (11)), thus the second term of (7) vanishes.

Solving (7) for δ as an asymptotic expansion in $\sqrt{\varepsilon}$ with the lowest term of $\mathcal{O}(\sqrt{\varepsilon})$ gives:

$$\delta = \gamma_1\sqrt{\varepsilon} + \gamma_2\varepsilon + \gamma_3\varepsilon^{3/2} + \mathcal{O}(\varepsilon^2), \tag{8}$$

where:

$$\gamma_1 = \sqrt{-\frac{\langle \nabla H_u, x_0 \rangle}{\langle \nabla H_u, \frac{\partial F_s}{\partial x} F_s \rangle}}. \tag{9}$$

Note that the analytical conditions for this case (see (4), (18) and (11)) guarantee that such asymptotic expansion is consistent.

Finally, substituting (8) into (5), we get the following expression for $\bar{x}$ (we shall consider terms up to $3/2$ terms):

$$\bar{x} = \sqrt{\varepsilon}\chi_1 + \varepsilon\chi_2 + \varepsilon^{3/2}\chi_3, \tag{10}$$

where:

$$\chi_1 = \gamma_1 F_s, \tag{11}$$

$$\chi_2 = x_0 + \gamma_2 F_s + \gamma_1^2 a_s, \tag{12}$$

$$\chi_3 = \gamma_3 F_s + 2\gamma_1\gamma_2 a_s + \gamma_1^3 c_s + \gamma_1 b_s x_0. \tag{13}$$

A.2 Second step

Having derived an expression for $\bar{x}$, now we need to consider the subsequent motion from $\bar{x}$. In particular, the system trajectory starting from $\bar{x}$ will evolve along the vector field F_1 for some time, say $-\delta$, until reaching the final point x_f.

Using again Taylor series expansion, we can get an approximate expression for $x_f = \phi_1(\bar{x}, -\delta)$ as:

$$\begin{aligned} x_f \quad &\approx \quad \bar{x} - \delta F_1 + \delta^2 a_1 - \delta b_1 \bar{x} - \delta^3 c_1 - \delta d_1 \bar{x}^2 \\ &\quad + \delta^2 e_1 \bar{x} + \delta^4 f_1 - \delta g_1 \bar{x}^3 + \delta^2 h_1 \bar{x}^2 - \delta^3 j_1 \bar{x}. \end{aligned} \tag{14}$$

Collecting terms at subsequent powers of ε will yield to the leading order:

$$\begin{aligned} x_f \approx (-\gamma_3 F + \chi_3 - (\chi_1\gamma_2 + \chi_2\gamma_1)b_1 + \chi_1 e_1 \gamma_1^2 - \chi_1^2 \gamma_1 d_1 + 2\gamma_1\gamma_2 a_1 - \gamma_1^3 c_1)\varepsilon^{3/2} + \\ + (\chi_2 + \gamma_1^2 a_1 - \gamma_2 F - \chi_1\gamma_1 b_1)\varepsilon + (\chi_1 - \gamma_1 F)\sqrt{\varepsilon}. \end{aligned} \tag{15}$$

It can be shown that the first two terms (at $\sqrt{\varepsilon}$ and ε) cancel out. Finally, we can write an approximate expression for x_f as:

$$x_f = \varepsilon x_0 + \gamma_1 \left(\frac{1}{3}(F_2 - F_1)\langle \nabla H_u, x_0 \rangle \right) \varepsilon^{3/2} + \mathcal{O}(\varepsilon^2). \tag{16}$$

Therefore, the ZDM in the current case can be expressed as:

$$D(x) = \begin{cases} x + M_1\mu + N_1\nu \qquad \text{when} \qquad \langle \nabla H_u, x_0 \rangle \geq 0 \\ x + \mathbf{v} + H.O.T. + M_1\mu + N_1\nu \qquad \text{when} \qquad \langle \nabla H_u, x_0 \rangle < 0 \end{cases} \tag{17}$$

with $\mathbf{v} = \gamma_1 \left(\frac{1}{3}(F_2 - F_1)\langle \nabla H_u, x_0 \rangle \right) \varepsilon^{3/2}$ and M_1, N_1 some column matrices.

References

[1] B. Brogliato. *Nonsmooth Mechanics.* Springer–Verlag, 1999.

[2] H. Dankowicz and A. B. Nordmark. On the origin and bifurcations of stick-slip oscillations. *Physica D*, 136:280–302, 1999.

[3] M. di Bernardo, C. J. Budd, and A. R. Champneys. Corner-collision implies border-collision bifurcation. *Physica D*, 154:171–194, 2001.

[4] M. di Bernardo, C. J. Budd, and A. R. Champneys. Unified framework for the analysis of grazing and border-collisions in piecewise-smooth systems. *Physical Review Letters*, 86(12):2554–2556, 2001.

[5] M. di Bernardo, C. J. Budd, and A.R. Champneys. Normal form maps for grazing bifurcations in n-dimensional piecewise-smooth dynamical systems. *Physica D*, 160:222–254, 2001.

[6] M. di Bernardo, M. I. Feigin, S.J. Hogan, and M. E. Homer. Local analysis of C-bifurcations in n-dimensional piecewise smooth dynamical systems. *Chaos, Solitons and Fractals*, 10:1881–1908, 1999.

[7] M. di Bernardo, F. Garofalo, L. Iannelli, and F. Vasca. Bifurcations in piecewise–smooth systems. *International Journal of Control*, 75(16):1243–1259, 2002.

[8] M. di Bernardo, K. H. Johansson, and F. Vasca. Self-oscillations in relay feedback systems: Symmetry and bifurcations. *International Journal of Bifurcations and Chaos*, 11:1121–1140, 2001.

[9] M. di Bernardo, P. Kowalczyk, and A. Nordmark. Classification of sliding bifurcations of periodic orbits in piecewise smooth dynamical systems. in preparation, 2002.

[10] M. di Bernardo, P. Kowalczyk, and A. Nordmark. Sliding bifurcations: a novel mechanism for the sudden onset of chaos in friction oscillators. Accepted for publication in International Journal of Bifurcations and Chaos, 2003.

[11] M. di Bernardo, P.Kowalczyk, and A.Nordmark. Bifurcations of dynamical systems with sliding: derivation of normal form mappings. *Physica D*, 170:175–205, 2002.

[12] M. I. Feigin. *Forced Oscillations in systems with discontinuous nonlinearities.* Nauka, Moscow, 1994. In Russian.

[13] P. Kowalczyk. *Analytical and Numerical investigation of sliding bifurcations in n-dimensional piecewise-smooth systems.* PhD thesis, University of Bristol, 2003.

[14] P. Kowalczyk. On codimension-two c bifurcations. Technical report, University of Bristol, 2003.

[15] P. Kowalczyk and M. di Bernardo. Existence of stable asymmetric limit cycles and chaos in unforced symmetric relay feedback systems. In *Proceedings of European Control Conference, Porto*, pages 1999–2004, 2001.

[16] P. Kowalczyk and M. di Bernardo. On a novel class of bifurcations in hybrid dynamical systems - the case of relay feedback systems. In *Proceedings of Hybrid Systems Computation and Control*, pages 361–374. Springer–Verlag, 2001.

[17] Y. A. Kuznetsov, S. Rinaldi, and A. Gragnani. One parameter bifurcations in planar Filippov systems. *In Preprints of Department of Mathematics, Universiteit Utrecht, The Netherlands*, 2002.

[18] A. B. Nordmark. Non-periodic motion caused by grazing incidence in impact oscillators. *Journal of Sound and Vibration*, 2:279–297, 1991.

[19] H. E. Nusse and J. A. Yorke. Border–collision bifurcations for piece-wise smooth one-dimensional maps. *International Journal of Bifurcation and Chaos*, 5:189–207, 1995.

[20] V. I. Utkin. *Sliding Modes in Control Optimization.* Springer-Verlag, Berlin, 1992.

List of Figures

1 Phase space topology of a system with discontinuous vector fields 3

2 The four possible bifurcation scenarios involving collision of a segment of the trajectory with the boundary of the sliding region $\partial\hat{\Sigma}^{-}$. (a) crossing-sliding; (b) grazing-sliding; (c) switching-sliding; (d) adding-sliding. 4

3 Classification tree of different degenerate codimension-2 sliding bifurcations 6

4 Segment of a trajectory undergoing degenerate sliding bifurcation Case I. At the bifurcation point, the trajectory crosses the switching manifold at the codimension two node denoted by the letter A in Fig. 4. Dashed curves denote projection of the vector field onto the switching manifold Σ. The local maximum of the vector field is clearly visible. 8

5 Qualitatively different types of trajectories around the codimension-2 bifurcation point 9
6 Segment of a trajectory undergoing degenerate codimension-2 sliding bifurcation scenario Case II. 10
7 Segment of a trajectory undergoing degenerate sliding bifurcations: Case III 10
8 Qualitatively different types of trajectories around the codimension-2 bifurcation point 11
9 Qualitatively different types of trajectories around the codimension-2 bifurcation point 12
10 Segment of a trajectory undergoing degenerate sliding bifurcations: Case IV 12
11 Qualitatively different types of trajectories around the codimension-2 bifurcation point 13
12 Phase space topology around the codimension-2 14
13 Codimension-1 grazing-sliding bifurcations unfolded from the codimension-2 node 15
14 Bifurcating trajectory in 3-dimensional phase space 20
15 Projection of the bifurcating trajectory onto time-space coordinates. x_1 denotes position and x_3 the time coordinate. 20
16 Boundaries in the phase space around the degenerate crossing codimension 2 node 23
17 Qualitatively different trajectories around the codimension-2 node starting from regions R_1, R_2 and R_3.Time series representing the velocity coordinate of the trajectories starting in every of the three regions are shown in each of the panels. Each panel is labelled with the letter indicating the starting point in phase space as shown in Fig. 16. 23
18 Construction of the ZDM in the degenerate Case I of sliding bifurcations: Mapping D 27